dx.doi.org/10.14227/DT300223P88

Biorelevant Dissolution Testing of Numerically Optimized Multiparticulate Drug Delivery Systems of Gliclazide

Ebtesam W. Elsayed[1*], Ahmed A. El-Ashmawy[1], Nadia M. Mursi[2], and Laila H. Emara[1]

[1]*Medicinal and Pharmaceutical Chemistry Department, Pharmaceutical and Drug Industries Research Institute, National Research Centre, Dokki, Giza, Egypt.*

[2]*Department of Pharmaceutics, Faculty of Pharmacy, Cairo University, Cairo, Egypt.*

e-mail: ebtesam.wahman@yahoo.com

ABSTRACT

Gliclazide (GLZ) is an ampholyte with pH-dependent solubility in the gastrointestinal pH range. Although the effects of different pH values on GLZ release have been thoroughly investigated in compendial dissolution media, the effects of gastrointestinal fluid components and pH are not well known. Multiple response optimization was carried out employing two optimization criteria to obtain different release profiles (optimized alginate-gelatin beads, OP-1 and OP-2). Thermograms indicated polymorph formation (OP-1) and changes in GLZ crystallinity (OP-2). Fourier transform infrared (FT-IR)-spectra confirmed GLZ chemical stability. GLZ release in gradient compendial and biorelevant media was studied employing two dissolution methodologies using fed state simulated gastric and intestinal fluid (FeSSGF and FeSSIF, respectively). A validated HPLC/UV method for GLZ analysis in biorelevant media was developed. OP-1 and OP-2 showed low relative error between the actual and predicted values. In the gradient biorelevant media, OP-1 showed faster GLZ release than OP-2. In the gradient compendial media, OP-1 showed slower GLZ release in pH 1.2 and faster release in pH 7.4 than OP-2. Generally, both formulations showed slower GLZ release in biorelevant compared to compendial media. SEM images of OP-1 showed tiny pores on the bead surface after GLZ release in biorelevant media. Meanwhile, thin polymer layers were diffused around the beads (OP-1 and OP-2) after GLZ release in compendial media. In conclusion, GLZ release was mainly affected by pH rather than media components. A cost-effective biorelevant dissolution methodology was proposed.

KEYWORDS: Gliclazide, biorelevant media, numerical optimization, gradient conditions, cost-effective methodology, dissolution

INTRODUCTION

Biorelevant dissolution tests enable understanding of how a drug is predicted to perform after administration. The test can be utilized during formulation development to predict the dissolution and bioavailability of many drugs (*1*). For some drugs, dissolution tests may be used to establish an in-vitro correlation for evaluating the in-vivo performance. In addition, they can predict the effect of food on the bioavailability of many drugs, especially poorly soluble ones (*2*, *3*). Compendial dissolution media are typically utilized for quality control tests. However, compendial media do not enable predicting the in vivo performance of poorly soluble compounds, as the composition of those media may not represent the physiological state of the gastrointestinal (GI) tract at the time of drug administration (i.e., fed or fasted condition) (*1*).

Simulating GI conditions with biorelevant media is performed in many laboratories; however, biorelevant media are expensive due to their complexity, and they should be freshly prepared directly before conducting the dissolution test, which limits widespread use (*4*, *5*). The International Pharmaceutical Federation (FIP) published two biorelevant media: fasted state simulated intestinal fluid (FaSSIF) and fed state simulated intestinal fluid (FeSSIF). FeSSIF contains bile salt and lecithin, with pH, buffer capacity, and osmolality of the intestine (*5*).

*Corresponding author

The conventional dissolution media contains synthetic surfactants that form micelles, whereas FeSSIF and FaSSIF contain natural surfactants that form more complex lipid aggregates (*3*). In these media, several properties are taken into consideration such as pH and bile salt concentration (*6*). For poorly soluble drugs, bile salts and phospholipids may significantly affect the drug dissolution and transport in the small intestine. There is a growing interest in the standardization of biorelevant dissolution methodology. Moreover, different studies have utilized pharmacokinetic modeling with biorelevant dissolution testing for the prediction of the in vivo behavior of many drugs (*7–10*).

For modified-release (MR) dosage forms, dissolution is a critical quality attribute. Drug release from these formulations should follow a predefined delivery pattern. MR dosage forms are exposed to changing conditions as they move through the GI tract, which can affect the drug release. Thus, it is necessary to establish drug release test conditions in a way that these effects can be observed and predicted using a series of media in one experiment (*11*). In a gradient dissolution test, the release profiles can be studied using the same settings with varying pH conditions to detect drug release changes that might occur by changing pH as the dosage form moves through the GI tract (*12*).

Gliclazide (GLZ) is a second-generation sulphonylurea used for the management of type II diabetes mellitus (*13*, *14*). It is a white crystalline powder, relatively insoluble in water (*15*). GLZ belongs to BCS class II drugs (low solubility and high permeability drugs), hence GLZ dissolution is the rate-limiting step for its absorption (*16–18*). It is a hydrophobic drug, a weak acid (pKa = 5.8), and it exhibits a pH-dependent solubility (*15*, *18–20*).

The aim of the current study was to investigate the GLZ release rate from two different numerically optimized multiparticulate drug delivery systems in both compendial and biorelevant media. The optimization criteria were considered to obtain different GLZ release patterns in different pH values. The study also focused on validating GLZ quantification methodology and establishing a cost-effective dissolution methodology in biorelevant media using gradient conditions.

METHODS

GLZ powder was donated from Sigma Pharmaceutical Industries, Menoufia, Egypt. For the preparation of alginate-gelatin (AL-GL) beads, high viscosity sodium alginate and gelatin (Bovine-B) from Sigma Aldrich (USA) and 50% w/w glutaraldehyde and anhydrous calcium chloride from ADWIC (Egypt) were used. HPLC-grade acetonitrile, ethyl acetate, and methanol from TEDIA (USA) were used. Hydrochloric acid (HCl) 30–34% (El-Nasr Pharmaceutical Chemicals Co., Egypt), potassium di-hydrogen phosphate (ADWIC), and sodium hydroxide pellets (Laboratory Rasayan, India) were used for the preparation of compendial media. Sodium chloride extra pure (NaCl) (Laboratory Rasayan, S. D. Fine-Chem Ltd., India), sodium acetate trihydrate (ADWIC), acetic acid 96% (ADWIC), taurocholic acid sodium salt (Aldrich Chemicals, USA), lecithin (≥ 97% for biochemistry, Roth, Germany), full cream UHT-milk (Juhayna, Egypt) were used to prepare the biorelevant media. Milli-Q purified water (Millipore Corp., Billerica, MA, USA) was used.

Multiple Response Optimization and Preparation of Alginate-Gelatin (AL-GL) Beads

Multiple response optimization was carried out based on a previous study; the optimized AL-GL beads were prepared according to that same study (*21*). Alginate and gelatin were dissolved in water (1:40 w/w ratio of polymer to distilled water). GLZ powder was quantitatively transferred to AL-GL solution while stirring, and the formed suspension was dropped on curing solutions using a peristaltic pump (falling distance was 7.5 cm, 3.5-mm tube [Rainin Dynamax, USA]). The curing solutions consisted of different concentrations of glutaraldehyde (GA, X3) in 0.2 M CaCl2 solution (w/v) kept at 5 ± 0.5 °C in a temperature-controlled circulator water bath (F20-VC, Julabo, Germany). The formed beads were kept in the curing solution while stirred for 30 min, then washed with distilled water and left to dry until reaching a constant weight. Blank beads (drug-free) were also prepared using the same method. The composition of the optimized AL-GL beads is summarized in Table 1.

Evaluation of the Optimized Beads

GLZ Loading and Incorporation Efficiency

For each formulation, accurately weighed beads corresponding to a theoretical weight of 20 mg of GLZ were ground to a powder and shaken in 250 mL of phosphate buffer (pH 7.4) for 24 h at 37 °C ± 0.5 (shaking water bath, Lab-Line, USA). Each sample was filtered through a 0.45-µm filter, diluted, and analyzed spectrophotometrically at 225 nm (Beckman, DU-650, USA). GLZ loading and incorporation efficiency (IE) were calculated according to the following equations (*22*):

GLZ loading % = (Drug weight in beads / weight of beads) x 100;

IE % = (Actual amount of drug in beads/ theoretical amount of drug in beads) x 100.

Table 1. Composition and Characteristics of OP-1 and OP-2

			OP-1 (*21*)	OP-2
Optimization criteria		Y_1: IE	Maximized	Maximized
		Y_2: (*Q* 0.5 h)	5% ≤ Y_2 ≤ 20%	20% ≤ Y_2 ≤ 30%
		Y_3: (*Q* 2 h)	15% ≤ Y_3 ≤ 25%	30% ≤ Y_3 ≤ 40%
		Y_4: (*Q* 4 h)	60% ≤ Y_4 ≤ 70%	50% ≤ Y_4 ≤ 60%
Desirability			1	1
Studied factors		X_1: GLZ%	17.94%	19.04%
		X_2: AL:GL	1:1	1:1
		X_3: GA%	0.1%	10.63%
Predicted responses		Y_1: IE	82.78%	70.14%
		Y_2: (*Q* 0.5 h)	7.86%	22.38%
		Y_3: (*Q* 2 h)	21.32%	33.51%
		Y_4: (*Q* 4 h)	68.46%	57.93%
Actual responses (mean ± SD, *n* = 3)		Y_1: IE	81.69 ± 3.98	70.15 ± 0.64
		Y_2: (*Q* 0.5 h)	7.98 ± 0.02	22.22 ± 0.62
		Y_3: (*Q* 2 h)	20.98 ± 0.17	35.94 ± 1.60
		Y_4: (*Q* 4 h)	67.43 ± 2.76	61.3 ± 2.15
Relative error		Y_1: IE	1.32%	-0.01%
		Y_2: (*Q* 0.5 h)	-1.53%	0.71%
		Y_3: (*Q* 2 h)	1.59%	-1.28%
		Y_4: (*Q* 4 h)	1.5%	-5.81%
Regression coefficient (r^2) of kinetic release models	**Biorelevant media**	Zero-order	0.9964	0.9822
		First-order	0.9568	0.9705
		Higuchi	0.9727	0.9299
		Hixson & Crowell	0.9817	0.9757
	Compendial media	Zero-order	0.9502	0.9875
		First-order	0.7102	0.9780
		Higuchi	0.8750	0.9474
		Hixson & Crowell	0.7033	0.9664

AL: alginate; IE: incorporation efficiency; GA: glutaraldehyde; GL: gelatin; GLZ: gliclazide; Q: drug release; X: factor; Y: response.

Differential Scanning Calorimetry (DSC)

The thermal behavior was investigated by DSC (DSC-50, Shimadzu, Japan) to evaluate the state of GLZ in different tested samples. Samples (5 mg) were weighed into aluminum pans (heated in a nitrogen atmosphere), using an empty pan as a reference. The thermal analysis was carried out using a heating ramp from 25–350 °C at a 10 °C per minute scale-up rate. A nitrogen purge (25 mL/min) was maintained.

Fourier Transform Infrared Analysis

The tested samples were ground and mixed thoroughly with potassium bromide (1:5 ratio of sample to KBr). The powder was compressed at a pressure of 5 tons for 5 min in a hydraulic press to form KBr disks. Scans were obtained at a resolution of 4 cm^{-1} (FT-IR-6100 spectrometer, Jasco, Japan) from 400–4000 cm^{-1}.

GLZ Release Studies

Dissolution Test in Compendial Media

The dissolution test in compendial media was carried out using USP apparatus 1 (rotating basket) (AT8-XTEND, Sotax, Switzerland). The dissolution medium was 900 mL of filtered and degassed 0.1 N HCl for 2 h, followed by 900 mL of phosphate buffer at pH 7.4, maintained at 100 rpm and 37.0 ± 0.5 °C. Samples were collected at specified time points (0.5-h intervals for up to 7 h), filtered through a 0.45-µm filter, replaced with fresh dissolution medium, and analyzed for GLZ content with a UV-visible spectrophotometer (Beckman, DU-650, USA) at 225 nm against the corresponding blank solution (*22*).

Preparation of Biorelevant Media

The composition of FeSSGF was previously described by Jantratid et al. (*23*). It consisted of 50% ultra-heat treated milk (UHT milk) used to simulate the fed gastric conditions

added to the blank simulated gastric medium (Table 2) (*23*). FeSSIF was previously reported by Klein (*24*). It consisted of bile salt (sodium taurocholic acid) and lecithin dissolved in a blank simulated intestinal medium (Table 2). Most of the components were simply dissolved in Milli-Q water except for lecithin, which required ultrasonication (Sonics, USA) to completely dissolve. Both FeSSIF and FeSSGF were freshly prepared for each experiment. The selected simulated colonic fluid (SCoF) was reported by Fotaki et al. (*1*). Acetate buffer was used to adjust the desired pH (5.8) and buffer capacity (Table 2).

Table 2. Composition of Biorelevant Media Used to Simulate Fed State Condition in Gastrointestinal Tract

Component	FeSSGF* (*23*)	FeSSIF (*24*)	SCoF (*1*)
Sodium taurocholate	-	15 mM	-
Lecithin	-	3.75 mM	-
Acetic acid	17.12 mM	8.65 g	170 mM
Sodium acetate	29.75 mM	-	-
Sodium chloride	237.02 mM	11.874 g	-
Sodium hydroxide	-	4.04 g	157 mM
Deionized water (qs add)	1L	1L	1L
pH	5	5	5.8

**Blank medium mixed with UHT milk (1:1).*
Dash (-) indicates not applicable.
FeSSGF: fed state simulated gastric fluid; FeSSIF: fed state simulated intestinal fluid; SCoF: simulated colonic fluid.

Modification and Validation of HPLC/UV Method for GLZ Quantification

For the determination of GLZ in FeSSGF and FeSSIF, several HPLC methods were investigated. The selected HPLC method was mainly guided by previously published methods (*22*, *25*).

Preparation of Standard Solutions

Each calibration standard was prepared by adding a calculated volume of suitable GLZ standard solution to 100 µL of drug-free medium (either FeSSGF or FeSSIF). The calibration standard concentrations ranged from 0.1–30 µg/mL GLZ. The internal standard (glyburide) was used in a concentration of 2.5 µg/mL.

Preparation of Samples

GLZ extracting solvent (ethyl acetate) was added to the calibration standard or dissolution sample. The solvent layer (containing GLZ) was separated and evaporated under a vacuum. The dried calibration standards and dissolution samples were then reconstituted with 150 µL of mobile phase directly before injection.

Chromatographic Conditions

The mobile phase was a mixture of filtered and degassed deionized water and acetonitrile (45:55, Millipore vacuum filtration system with membrane filter, 0.45 µm) pumped at a flow rate of 1 mL/min with isocratic elution. The sample run time was 6 minutes. The UV detection wavelength was 230 nm. HPLC apparatus consists of: Waters 600 E Multi Solvent Delivery System Controller equipped with Rheodyne injector P/N 7725i, and Waters 2487 Dual λ Absorbance Detector coupled to Millennium 32 computer program. Column (Lichrosorb RP-18, 10 µm, 250 x 4.6 mm i.d., Merck, Germany) was kept at room temperature, protected by a guard column (Perisorb 30-40, Merck).

Dissolution Tests in Biorelevant Media

Two different dissolution test methods were investigated: USP apparatus 1 (rotating basket) and shaking water bath, a cost-effective alternative method.

USP Apparatus 1

The first dissolution medium was 900 mL of FeSSGF for 2 h, followed by 900 mL of FeSSIF for 3.5 h, followed by 900 mL of SCoF for 8 h. Each medium was maintained at 100 rpm and 37.0 ± 0.5 °C. The baskets were loaded with a weight of beads corresponding to 60 mg of GLZ. Samples were collected at specified time points (every 0.5 h for the first 6 h then every 1 h until 14 h), filtered through a 0.45-µm filter, replaced with fresh dissolution medium, and analyzed for GLZ content.

Shaking Water Bath

A shaking water bath was maintained at 37.0 ± 0.5 °C and 100 rpm. Glass stoppered 50-mL conical flasks were filled with 25 mL of each dissolution medium (2.78% of the official volume and the weight of beads was adjusted using the same factor) as follows. First, FeSSGF was added for 2 h, followed by FeSSIF for 3.5 h, followed by SCoF for 8 h. Samples were collected at specified time points (every 0.5 h for the first 6 h then every 1 h until 14 h), filtered through 0.45-µm filter, and replaced with fresh dissolution medium.

For analytical purposes, the same tests were carried out using blank beads (drug-free) and samples were collected at the same time intervals. The collected samples were analyzed for GLZ content using the validated HPLC/UV method (for FeSSGF and FeSSIF samples) and UV/spectrophotometric method at 225 nm (for SCoF samples).

Mathematical Comparison of GLZ Release Profiles

Release profiles of GLZ were compared using the fit factors f_1 and f_2 (*26*). A difference factor, f_1, between 0 and 15 ensures a minor difference between two products, and a similarity factor, ƒ2, between 50 and 100 ensures similar dissolution profiles (*26*). Dissolution efficiency (DE) was also calculated from the area under the dissolution

curve at time (t), measured using the trapezoidal rule, and expressed as a percentage of the area of the rectangle described by 100% dissolution at the same time (*26*).

Fitting to different kinetic release models was also evaluated. Zero-order release model, First-order release model, Higuchi square root of time model, and Hixson–Crowell cube root model were assessed (*21*).

Scanning Electron Microscopic (SEM) Analysis

SEM (Quanta GEF, Netherlands) imaging before and after GLZ release was performed and analyzed.

RESULTS AND DISCUSSION

Multiple Response Optimization and Evaluation of the Optimized Formulations

Multiple response optimization was carried out based on previously published work (*21*). A three-factor three-level face-centered design (FCD) was implemented where GLZ%, AL:GL ratio, and glutaraldehyde (GA)% were the studied factors (X_1, X_2, and X_3, respectively). The studied responses were GLZ IE and release (Q) after 0.5 h, 2 h, and 4 h (Y_1: IE, Y_2: Q 0.5 h, Y_3: Q 2 h, and Y_4: Q 4 h, respectively). After a comprehensive evaluation of the regression models, two different optimization criteria were employed (OP-1 and OP-2) (Table 1). Noticing that increasing GA% resulted in faster GLZ release in the acidic medium (pH 1.2) and a slower release in phosphate buffer (pH 7.4) in addition to its significant negative effect on IE, the numerical optimization was utilized to obtain different suggested solutions (formulations) with the highest desirability. The objective of the optimization criteria was to obtain two formulations; one of them enables faster drug release in 0.1 N HCl pH 1.2 (OP-2) and the other enables faster drug release in phosphate buffer pH 7.4 (OP-1) (*21*).

In the current study, the optimized formulation (OP-2) was prepared based on numerical optimization (*27*). The optimization criteria for OP-2 were to maximize GLZ IE (Y_1), while GLZ release responses were specified with constraints ($20\% \leq Y_2 \leq 30\%$, $30\% \leq Y_3 \leq 40\%$, $50\% \leq Y_4 \leq 60\%$). The selected optimized formulations showed a desirability of 1. The relative error values for OP-1 and OP-2 were low, confirming the validity of the model (*28*, *29*) (Table 1).

Characterization of the Optimized Beads

Both OP-1 and OP-2 beads showed white color that changed to either yellow color (OP-1) or yellowish-brown color (OP-2) after drying. It was observed that the darker beads' color is linked to the higher concentration of GA (*21*). OP-1 and OP-2 beads were spherical before drying; however, due to the mild stickiness of OP-1 beads, their shape was less regular than OP-2 after drying. This could be attributed to incomplete cross-linking of gelatin as a result of using lower GA concentration (*21*). This effect was reflected in the coefficient of variation (CV% = 15.2 and 6.3 for OP-1 and OP-2, respectively).

Thermograms

DSC studies were carried out for pure GLZ, pure polymers, blank beads, and GLZ-loaded beads (Fig. 1A). DSC-thermogram of blank OP-2 beads (drug-free) showed a broad endothermic peak at 91.54 °C and disappearance of the exothermic peak of alginate as a result of its crosslinking and/or interaction between alginate and gelatin. This thermal behavior was also observed in blank OP-1 beads (*21*). Thermogram of GLZ-loaded OP-2 beads showed disappearance of a GLZ endothermic peak, which might indicate a change in the crystallinity of GLZ (*30*). Loss of crystallinity might enhance the drug dissolution; however, this effect was not observed in the current study. This could be attributed to the delay of GLZ wetting by crosslinked polymers, hence slowing GLZ release (*21*). In contrast, the thermogram of GLZ-loaded OP-1 beads showed endothermic peaks at 152.78 °C and 163.07 °C. This indicates formation of GLZ polymorphs (*21*).

FTIR Analysis

FTIR analysis was carried out for pure GLZ, pure polymers, blank beads, and GLZ-loaded beads (Fig. 1B). Both blank OP-1 and blank OP-2 beads (drug-free) showed amide carbonyl stretch peaks at 1629.55 cm^{-1} that indicated amide bond formation between the amino group of gelatin and the carboxylic group of gelatin or alginate (*31*, *32*). The FTIR spectra of GLZ-loaded OP-1 and OP-2 beads showed asymmetric sulfonyl (S=O) stretching peak at 1348 cm^{-1} and symmetric sulfonyl (S=O) stretching peak at 1162.87 cm^{-1}. The amide carbonyl stretch peak at 1631.48 cm-1 was also observed. The observed peaks are characteristic for GLZ, so no chemical change was indicated.

Selection Criteria of Biorelevant Media

The selected biorelevant medium simulating the fed state gastric condition is composed of a mixture of blank gastric medium and UHT milk in a ratio of 1:1 as previously proposed (*23*) (Table 2). FeSSGF should simulated the physicochemical properties of a standard meal while being experimentally practical (*24*, *33*). Standardized homogenized cows' whole milk is similar to a standard breakfast meal with regard to the ratio of the components, pH, and physicochemical properties (*24*). As the stability of fresh milk at 37 °C is challenging, UHT milk was used. The brand and quality of milk were standardized to avoid variation in its composition (*24*).

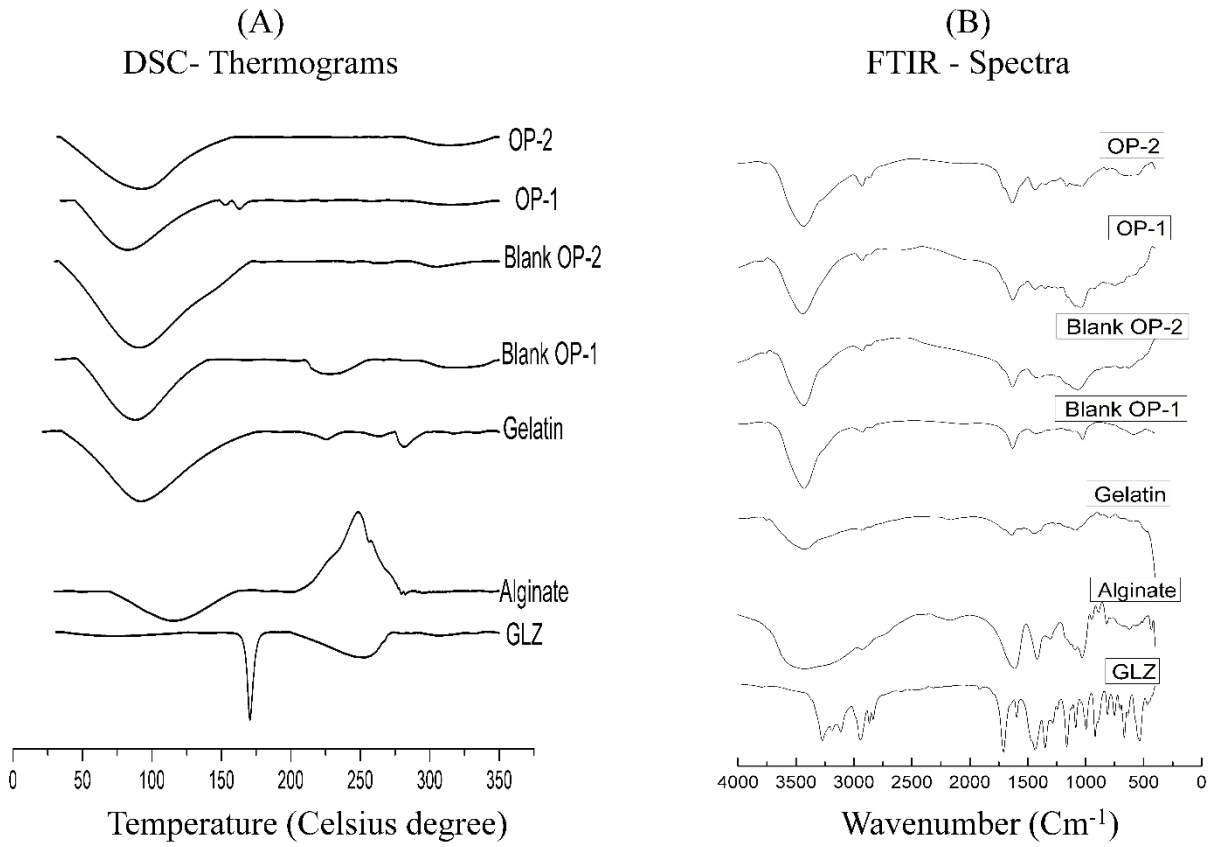

Figure 1. Physicochemical characterization of gliclazide (GLZ) optimized formulations (OP-1 and OP-2): DSC-thermograms (A) and FTIR spectra (B) of GLZ, sodium alginate (high viscosity), gelatin (Bovine-B), GLZ-loaded, and blank optimized beads. DSC: differential scanning calorimetry; FTIR: Fourier transform infrared.

The selected biorelevant medium simulating the intestinal conditions in the fed state (Table 2) was as proposed by Klein (*24*). It contained molar ratios of sodium taurocholate and lecithin that simulate the in-vivo ones. The composition of the intestinal fluid is also dependent on the type of the ingested meal, though, to a lower extent than the gastric fluid. Food-induced bile secretion increases bile salt levels in the small intestine between 8 and 20 mM up to 40 mM (*33*, *34*). The ratio between bile salts and phospholipids depends on the phospholipid concentration present in food. It is reported to range from 2:1 to 5:1 (*33*, *35*). FeSSIF composition was first proposed by Dressman et al. (*36*). It simulates the intestinal fluid regarding bile salt, phospholipids in addition to pH, osmolarity, and buffer capacity (*33*). The FeSSIF proposed by Dressman et al. included acetic acid and potassium chloride for buffer capacity and osmolarity adjustment instead of acetic acid, sodium acetate, and sodium chloride in the medium proposed by Klein (*24*). Generally, the preparation methods of biorelevant media require emulsification in a chlorinated solvent or may involve sequential addition. The preparation method in this study was simple and does not require the addition of a chlorinated solvent.

The selected SCoF medium composition was proposed by Fotaki et al. (*37*) (Table 2). Generally, the development of SCoF is mainly dependent on pH and short-chain fatty acid concentrations. Acetate buffer was used to adjust the desired pH (5.8) and buffer capacity (*1*).

Residence Time in the Gastrointestinal Tract

In this study, FeSSGF was used for 2 hours, then replaced with FeSSIF for 3.5 hours, which was finally replaced with SCoF for 8 hours. Dimensions of the dosage form drastically affect the residence time. Moreover, gastric emptying is faster in the fasted state than in the fed state causing the dosage form to reach the higher pH regions of the intestine rapidly. The gastric residence time is usually shorter for multiparticulate systems than for single-unit systems (*11*, *38–40*). However, the spherical shape makes it easier for beads to reach the colon and retain in the ascending colon. This supports the longer duration of action of beads (*41*). Jantratid et al. (*11*) suggested the residence times of pellets in different regions of the GI tract based on the literature data and applied them to diclofenac sodium MR pellet biorelevant dissolution tests (*11*). The proposed residence times of pellets were utilized in the current study.

Quantification of GLZ in the Biorelevant Media

The complexity of the composition of the biorelevant media necessitates the validation of drug analytical methods to ensure obtaining reliable and reproducible results. It is difficult to establish an analytical method to accurately quantify a drug in milk-based media (FeSSGF) as the drug may distribute into different phases of milk. Jantratid et al. used the 'infinity point' approach (*11*). The limitation of this approach is that it does not give enough data about the dissolution rate in the FeSSGF as it estimates the total amount of drug dissolved at the end of this phase. For accurate quantification of GLZ in biorelevant media using the gradient conditions, the analytical method was modified and validated.

HPLC/UV Method Validation for Quantification of GLZ in FeSSGF and FeSSIF

The HPLC chromatograms revealed that GLZ was eluted at 4.3 minutes and the internal standard (IS) was eluted at 5.5 minutes. No interfering peaks were detected neither from the biorelevant media nor the blank beads. This indicates good resolution and selectivity (Fig. 2).

Two HPLC calibration curves at 230 nm were constructed by plotting GLZ/glyburide peak area ratio against GLZ concentrations in the ranges of 0.5–5 µg/mL and 5–60 µg/mL for each biorelevant medium. Linear relationships were established between GLZ standard concentrations and (GLZ/glyburide) peak areas ratio.

In FeSSGF, the coefficients of determination (r^2) were found to be 0.9986 and 0.9988 for the calibration curves of the lower concentrations and the higher concentrations, respectively. The response factors (procedural constant) were found to have mean values of 0.39 ± 0.03 and 0.42 ± 0.043 for the lower concentrations and the higher concentrations, respectively, with a relative standard deviation (RSD) less than 10%.

In FeSSIF, the r^2 values were 0.9937 and 0.9968 for the calibration curves of the lower concentrations and the higher concentrations, respectively. The response factors (procedural constant) were found to have mean values of 0.216 ± 0.032 and 0.33 ± 0.042 for the lower concentrations and the higher concentrations, respectively, with RSD less than 15%.

Three replicates of the samples spiked with different amounts of GLZ (covering the range of 0.5–60 µg/mL) were analyzed. The accuracy was measured as the mean percentage recovery. The recovery ranged from 90–109% for the standard concentrations in FeSSGF and from 90–105% for the standard concentrations in FeSSIF.

The analytical precision was determined by the CV% of the peak area ratios, which ranged from 4.2–12.21% for the standard concentrations in FeSSGF and from 2.3–11.28% for the standard concentrations in FeSSIF.

Comparative Dissolution of GLZ in Biorelevant Media

In the current study, two different dissolution methods were investigated. The main objective was to establish a reliable cost-effective methodology and to utilize the flexibility and reproducibility of the drug release data that can be obtained from the multiparticulate drug delivery systems. As GLZ is administered with food (*42*, *43*), it is

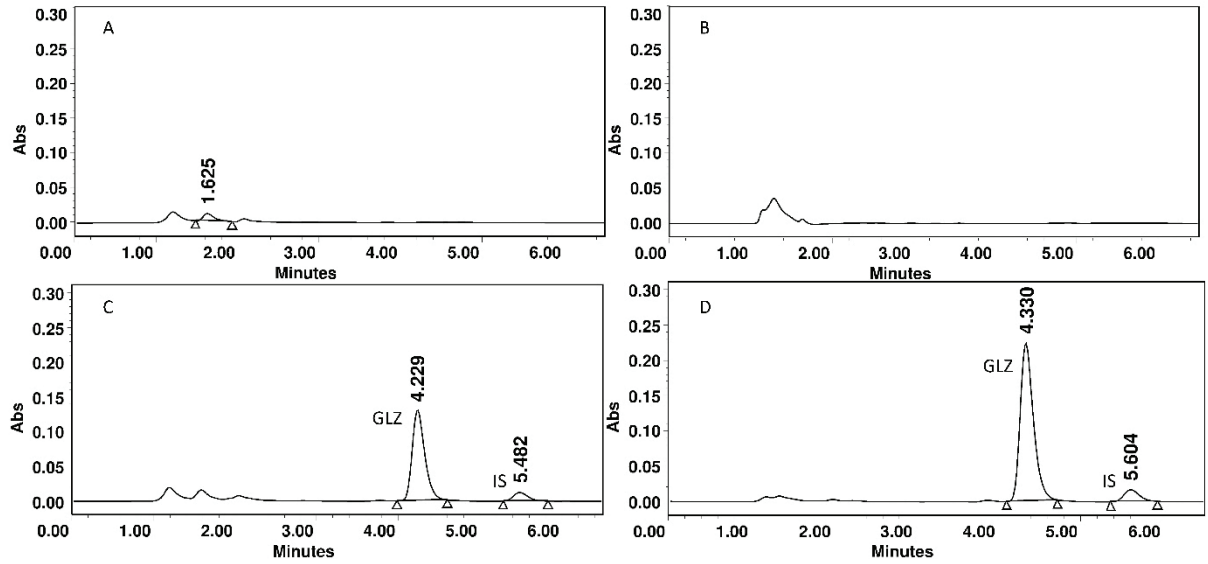

Figure 2. High-performance liquid ultraviolet chromatograms of blank FeSSGF (A), blank FeSSIF (B), GLZ with IS in FeSSGF (C), and GLZ with IS in FeSSIF (D). FeSSGF: fed state simulated gastric fluid; FeSSIF: fed state simulated intestinal fluid; GLZ: gliclazide; IS: internal standard; Abs: absorbance.

important to study its dissolution in the simulated fed state using gradient conditions.

The excellent weight-dose proportionality of the multiparticulate drug delivery systems enabled the reduction of biorelevant media volume to 25 mL instead of 900 mL (official volume). Figure 3A shows that the optimized AL-GL beads showed similar reproducible GLZ release patterns using USP apparatus 1 and the shaking water bath (f_2 = 72 and 79, f_1= 9 and 11 for OP-1 and OP-2, respectively). Both OP-1 and OP-2 showed slower release rates of GLZ in biorelevant media compared to the compendial media (Fig. 3). This was attributed to the physicochemical properties of GLZ, which is a weak acid with pH-dependent solubility (*15*, *18*). It is an ampholyte with a pH-dependent solubility in the GI pH range (*19*). Although its solubility is higher in the alkaline media, it has a reasonable solubility value in pH (1.2) that is comparable to its solubility in pH (7.4). However, GLZ shows very low solubility in the pH range of 2.5–6.5. Skripnik et al. studied GLZ release from MR GLZ tablets (market products) in different dissolution conditions (*44*). They used a ready-made biorelevant medium prepared as half-FaSSIF (fasted-state simulated intestinal fluid). In their study, complete drug release was achieved with apparatus 2 at 100 rpm, phosphate buffer (pH 6.8), during 24 h. However, half FaSSIF (pH 6.8), showed similar results to those obtained with phosphate buffer pH 6.8. Patel et al. also studied the effect of the bile salts, lecithin, and surfactants content in the ready-made FeSSIF powder (prepared in phosphate buffer pH 7.4) GLZ release (*45*). They concluded that the dissolution of GLZ was not affected by the content of biorelevant media while it might be affected by the simulated pH value itself, which was not studied (*45*, *46*). In the current study, the pH of biorelevant media was adjusted to simulate the fed-state conditions. The results indicated a pronounced effect of pH on GLZ release in both biorelevant and compendial media.

OP-1 showed faster GLZ release in all biorelevant media (FeSSGF, FeSSIF, and SCoF) compared to OP-2 (DE = 43.63% and 24.32%, respectively). About 83% of GLZ was released from OP-1 after 14 hours compared to 50% from OP-2 (Fig. 3A). On the other hand, GLZ release from OP-1 was slower than OP-2 in 0.1 N HCl (pH 1.2, DE 2h = 10.19% and 26.73%, respectively), and it was faster in pH 7.4 (Fig. 3B). This release pattern was accurately predicted based on the previously implemented design of experiments and response surface methodology (*21*).

Both OP-1 and OP-2 showed a zero-order GLZ release pattern in the compendial and biorelevant media (Table 1). Zero-order release refers to systems where the drug release rate does not depend on the concentration (*47*). These results suggested that the reservoir system of AL-GL beads was not affected by the biorelevant media while slower release patterns were obtained.

This is the first study that investigates GLZ release from a multiparticulate drug delivery system in fed-state

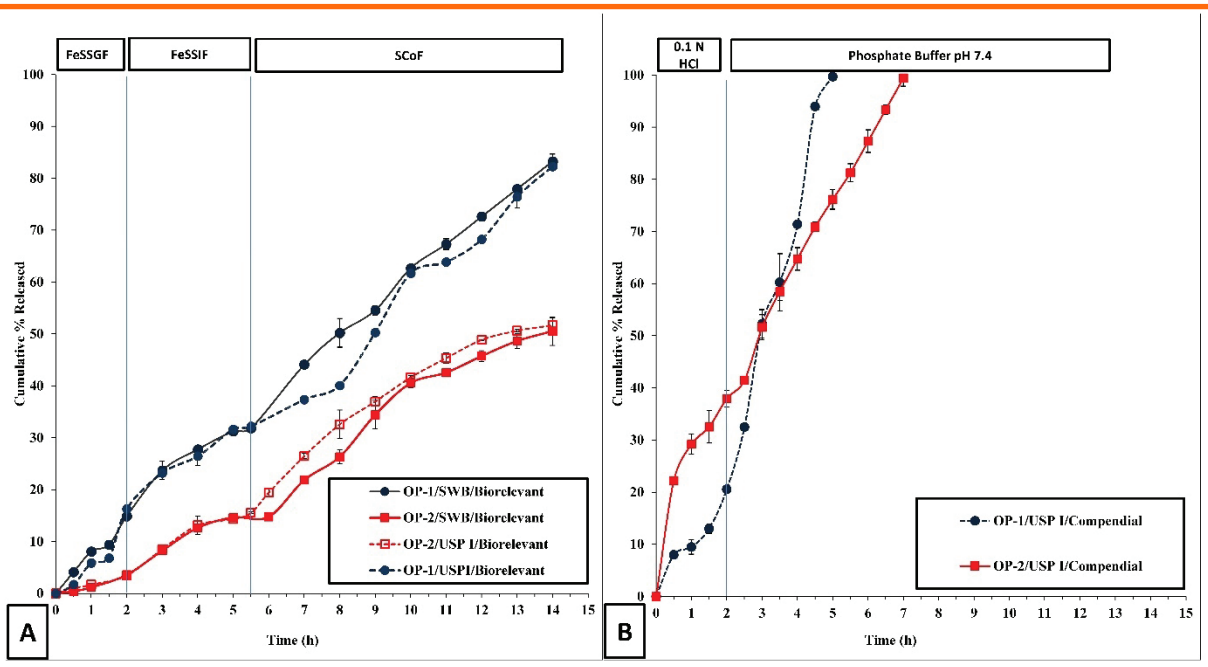

*Figure 3. Cumulative release of gliclazide (%) from optimized formulations (OP-1 and OP-2) in biorelevant media employing USP I apparatus and shaking water bath (SWB) (**A**) and in compendial media (**B**). FeSSGF: fed state simulated gastric fluid; FeSSIF: fed state simulated intestinal fluid; SCoF: simulated colonic fluid; HCl: hydrochloric acid.*

biorelevant media applying gradient conditions. The cost-effective methodology was mainly dependent on the excellent weight dose proportionality of the multiparticulate drug delivery systems that enabled the reduction of the biorelevant media volume to 25 ml instead of 900ml. Furthermore, the biorelevant media were prepared from their components and the preparation method was simple and does not require the addition of a chlorinated solvent as frequently carried out.

Scanning Electron Microscope (SEM)

Figure 4 shows OP-1 and OP-2 beads integrity (X 100) and surface topography (X 3000) before and after GLZ release. For OP-1 beads, a thin layer of crosslinked polymers diffused around the bead after GLZ release in compendial media suggests a change in the crosslinked polymers, and no pores were observed on the surface (Fig. 4B). After GLZ release in biorelevant media from OP-1 beads, no change was observed in the integrity of beads but there were numerous tiny pores on the surface (Fig. 4C); these pores were suspected to be responsible for GLZ release out of the beads. OP-2 beads integrity was drastically affected after GLZ release in compendial media. A widely diffused thin layer of the polymers was observed, and no pores were observed on the surface (Fig. 4B). After GLZ release in biorelevant media from OP-2 beads, no change was observed in the integrity of the bead, but the surface showed peeling of thin layers or flakes of the crosslinked polymers (Fig. 4C). The transverse sections of OP-1 and OP-2 beads showed no drug particles retained after GLZ release in compendial media (Figs. 4D and 4E). However, some drug particles were observed in the core of OP-1 and OP-2 beads after GLZ release in the biorelevant media (Figs. 4F and 4G); this was attributed to the slower drug release rate obtained in biorelevant media.

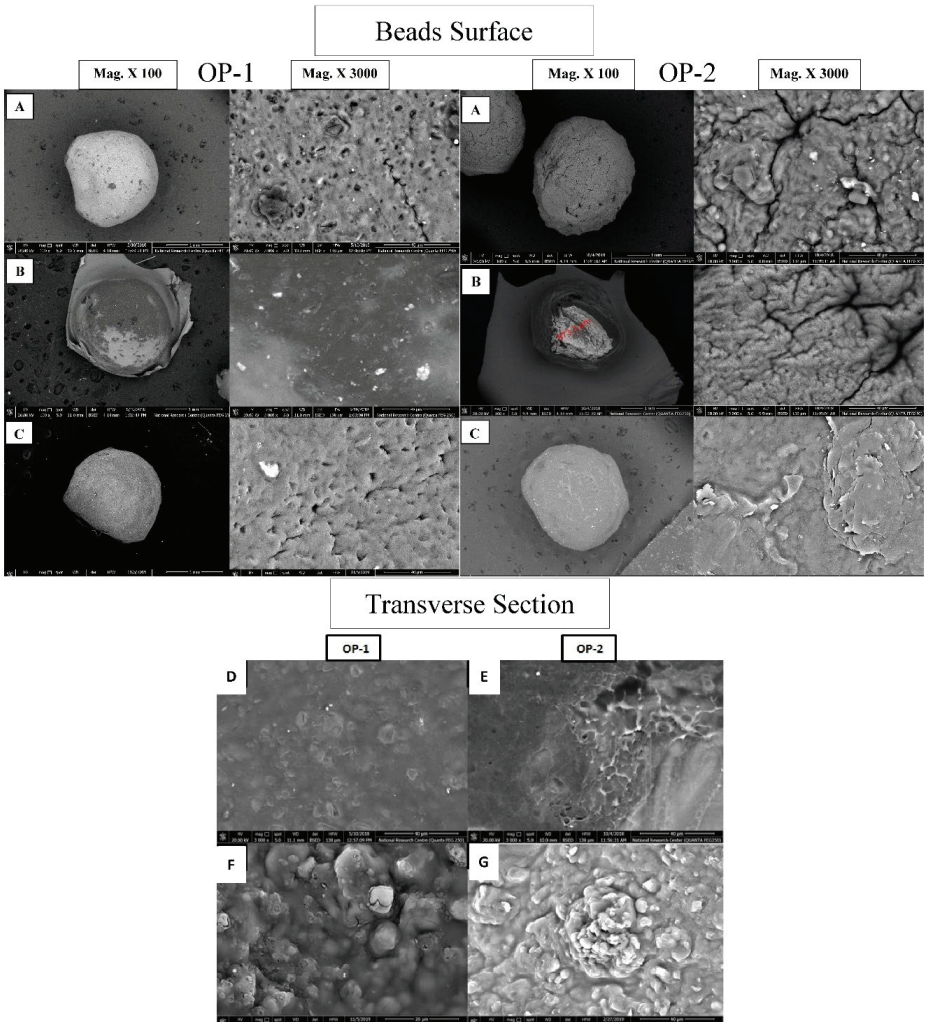

*Figure 4. Scanning electron microscope images of the optimized formulations (OP-1 and OP-2 beads) before GLZ release (**A**), bead surface after GLZ release in compendial media and biorelevant media (**B** and **C**, respectively), and transverse section of beads after GLZ release in compendial media (**D** and **E**) and biorelevant media (**F** and **G**).*

CONCLUSION

The current study indicated the pronounced effect of pH on GLZ release in both biorelevant and compendial media. This effect was reflected on the bead integrity and surface topography. GLZ release from AL-GL beads in biorelevant media was slower than its release in compendial media. The optimized formulation, OP-1, showed faster GLZ release than OP-2 in biorelevant media and phosphate buffer pH 7.4.

This is the first study that investigates GLZ release from a multiparticulate drug delivery system in fed-state biorelevant media applying gradient conditions. In addition, the methodology was much more cost-effective compared to the ready-made media in terms of the cost of components and ease of preparation.

CONFLICT OF INTEREST

The authors disclosed no conflicts of interest related to this article.

REFERENCES

1. Fotaki, N.; Vertzoni, M. Biorelevant dissolution methods and their applications in in vitro-in vivo correlations for oral formulations. *Open Drug Deliv. J*. **2010**, *4* (1), 2–13. DOI: 10.2174/1874126601004010002.
2. Nicolaides, E.; Galia, E.; Efthymiopoulos, C.; Dressman, J. B.; Reppas, C. Forecasting the in vivo performance of four low solubility drugs from their in vitro dissolution data. *Pharm. Res*. **1999**, *16* (12), 1876–1882. DOI: 10.1023/A:1018959511323.
3. Kloefer, B.; van Hoogevest, P.; Moloney, R.; Kuentz, M.; Leigh, M. L.; Dressman, J. Study of a standardized taurocholate-lecithin powder for preparing the biorelevant media FeSSIF and FaSSIF. *Dissolut. Technol*. **2010**, *17* (3), 6–13. DOI: 10.14227/DT170310P6.
4. Zoeller, T.; Klein, S. Simplified biorelevant media for screening dissolution performance of poorly soluble drugs. *Dissolut. Technol* **2007**, *14* (4), 8–13. DOI: 10.14227/DT140407P8.
5. Shekhawat, P. B.; Pokharkar, V. B. Understanding peroral absorption: regulatory aspects and contemporary approaches to tackling solubility and permeability hurdles. *Acta Pharm. Sin. B* **2017**, *7* (3), 260–280. DOI: 10.1016/j.apsb.2016.09.005.
6. Fang, J. B.; Robertson, V. K.; Rawat, A.; Flick, T.; Tang, Z. J.; Cauchon, N. S.; McElvain, J. S. Development and application of a biorelevant dissolution method using USP apparatus 4 in early phase formulation development. *Mol. Pharm*. **2010**, *7* (5), 1466-1477. DOI: 10.1021/mp100125b.
7. Loisios-Konstantinidis, I.; Cristofoletti, R.; Fotaki, N.; Turner, D. B.; Dressman, J. Establishing virtual bioequivalence and clinically relevant specifications using in vitro biorelevant dissolution testing and physiologically-based population pharmacokinetic modeling. case example: Naproxen. *Eur. J. Pharm. Sci*. **2020**, *143*, 105170. DOI: 10.1016/j.ejps.2019.105170.
8. Kambayashi, A.; Kiyota, T.; Fujiwara, M.; Dressman, J. B. PBPK modeling coupled with biorelevant dissolution to forecast the oral performance of amorphous solid dispersion formulations. *Eur. J. Pharm. Sci*. **2019**, *135*, 83–90. DOI: 10.1016/j.ejps.2019.05.013.
9. Kaur, N.; Narang, A.; Bansal, A. K. Use of biorelevant dissolution and PBPK modeling to predict oral drug absorption. *Eur. J. Pharm. Biopharm*. **2018**, *129*, 222–246. DOI: 10.1016/j.ejpb.2018.05.024.
10. Ibarra, M.; Valiante, C.; Sopeña, P.; Schiavo, A.; Lorier, M.; Vázquez, M.; Fagiolino, P. Integration of in vitro biorelevant dissolution and in silico PBPK model of carvedilol to predict bioequivalence of oral drug products. *Eur. J. Pharm. Sci*. **2018**, *118*, 176–182. DOI: 10.1016/j.ejps.2018.03.032.
11. Jantratid, E.; De Maio, V.; Ronda, E.; Mattavelli, V.; Vertzoni, M.; Dressman, J. B. Application of biorelevant dissolution tests to the prediction of in vivo performance of diclofenac sodium from an oral modified-release pellet dosage form. *Eur. J. Pharm. Sci.* **2009**, *37* (3-4), 434–441. DOI: 10.1016/j.ejps.2009.03.015.
12. Klein, S.; Dressman, J. B. Comparison of drug release from metoprolol modified release dosage forms in single buffer versus a pH-gradient dissolution test. *Dissolut. Technol*. **2006**, *13* (1), 6–12. DOI: 10.14227/DT130106P6.
13. Lebovitz, H.; Feinglos, M. *Diabetes Mellitus: Theory and Practices*. Medical Examination Publishing, 1983.
14. Parvez, M.; Arayne, M. S.; Zaman, M. K.; Sultana, N. Gliclazide. *Acta Crystallogr., Sect. C: Cryst. Struct. Commun*. **1999**, *55* (1), 74–75. DOI: 10.1107/S0108270198009883.
15. Biswal, S.; Sahoo, J.; Murthy, P. N.; Giradkar, R. P.; Avari, J. G. Enhancement of dissolution rate of gliclazide using solid dispersions with polyethylene glycol 6000. *AAPS PharmSciTech* **2008**, *9* (2), 563–570. DOI: 10.1208/s12249-008-9079-z.
16. Priya, M.; Murthy, T. Development of discriminative dissolution media for marketed gliclazide modified-release tablets. *Dissolut. Technol*. **2012**, *19* (2), 38–42. DOI: 10.14227/DT190212P38.
17. Amidon, G. L.; Lennernäs, H.; Shah, V. P.; Crison, J. R. A theoretical basis for a biopharmaceutic drug classification: the correlation of in vitro drug product dissolution and in vivo bioavailability. *Pharm. Res*. **1995**, *12* (3), 413–420. DOI: 10.1023/A:1016212804288.
18. Ambrogi, V.; Perioli, L.; Ciarnelli, V.; Nocchetti, M.; Rossi, C. Effect of gliclazide immobilization into layered double hydroxide on drug release. *Eur. J. Pharm. Biopharm*. **2009**, *73* (2), 285–291. DOI: 10.1016/j.ejpb.2009.06.007.
19. Grbic, S.; Parojcic, J.; Ibric, S.; Djuric, Z. In vitro–in vivo correlation for gliclazide immediate-release tablets based on mechanistic absorption simulation. *AAPS PharmSciTech* **2011**, *12* (1), 165–171. DOI: 10.1208/s12249-010-9573-y.
20. Schönherr, D.; Wollatz, U.; Haznar-Garbacz, D.; Hanke, U.; Box, K. J.; Taylor, R.; Ruiz, R.; Beato, S.; Becker, D.; Weitschies, W. Characterisation of selected active agents regarding pKa values, solubility concentrations and pH profiles by SiriusT3. *Eur. J. Pharm. Biopharm*. **2015**, *92*, 155–170. DOI: 10.1016/j.

ejpb.2015.02.028.
21. Elsayed, E. W.; El-Ashmawy, A. A.; Mursi, N. M.; Emara, L. H. Optimization of gliclazide loaded alginate-gelatin beads employing central composite design. *Drug Dev. Ind. Pharm*. **2019**, *45* (12), 1959–1972. DOI: 10.1080/03639045.2019.1689992.
22. Elsayed, E. W.; El-Ashmawy, A. A.; Mahmoud, K. M.; Mursi, N. M.; Emara, L. H. Modulating gliclazide release and bioavailability utilizing multiparticulate drug delivery systems. *J Pharm. Innov*. **2021**, *17*, 674–689. DOI: 10.1007/s12247-021-09542-9.
23. Jantratid, E.; Janssen, N.; Chokshi, H.; Tang, K.; Dressman, J. B. Designing biorelevant dissolution tests for lipid formulations: case example – lipid suspension of RZ-50. *Eur. J. Pharm. Biopharm*. **2008**, *69* (2), 776–785. DOI: 10.1016/j.ejpb.2007.12.010.
24. Klein, S. The use of biorelevant dissolution media to forecast the in vivo performance of a drug. *AAPS J*. **2010**, *12* (3), 397–406. DOI: 10.1208/s12248-010-9203-3.
25. Taha, N. F.; Elsayed, E. W.; El-Ashmawy, A. A.; Abdou, A. R.; Emara, L. H. Impact of sample storage conditions on gliclazide quantification in rat plasma by UHPLC/UV method: storage recommendation and pharmacokinetic application. *J. Appl. Pharm. Sci*. **2021**, *11* (3), 46–53. DOI: 10.7324/JAPS.2021.110305.
26. Costa, P.; Sousa Lobo, J. M. Modeling and comparison of dissolution profiles. *Eur. J. Pharm. Sci*. **2001**, *13* (2), 123–133. DOI: 10.1016/S0928-0987(01)00095-1.
27. Mundada, P. K.; Sawant, K. K.; Mundada, V. P. Formulation and optimization of controlled release powder for reconstitution for metoprolol succinate multi unit particulate formulation using risk based QbD approach. *J. Drug Deliv. Sci. Technol*. **2017**, *41*, 462–474. DOI: 10.1016/j.jddst.2017.09.001.
28. Sankalia, M. G.; Mashru, R. C.; Sankalia, J. M.; Sutariya, V. B. Reversed chitosan-alginate polyelectrolyte complex for stability improvement of alpha-amylase: optimization and physicochemical characterization. *Eur. J. Pharm. Biopharm*. **2007**, *65* (2), 215–232. DOI: 10.1016/j.ejpb.2006.07.014.
29. Vijayalakshmi, P.; Devi, V. K.; Narendra, C.; Srinagesh, S. Development of extended zero-order release gliclazide tablets by central composite design. *Drug Dev. Ind. Pharm*. **2008**, *34* (1), 33–45. DOI: 10.1080/03639040701386129.
30. Jondhale, S.; Bhise, S.; Pore, Y. Physicochemical investigations and stability studies of amorphous gliclazide. *AAPS PharmSciTech* **2012**, *13* (2), 448–459. DOI: 10.1208/s12249-012-9760-0.
31. Devi, N.; Hazarika, D.; Deka, C.; Kakati, D. Study of complex coacervation of gelatin A and sodium alginate for microencapsulation of olive oil. *J. Macromol. Sci. Part A* **2012**, *49* (11), 936–945. DOI: 10.1080/10601325.2012.722854.
32. Xing, Q.; Yates, K.; Vogt, C.; Qian, Z.; Frost, M. C.; Zhao, F. Increasing mechanical strength of gelatin hydrogels by divalent metal ion removal. *Sci. Rep*. **2014**, *4* (1), 4706. DOI: 10.1038/srep04706.
33. MüLLERTZ, A. Biorelevant dissolution media. In *Solvent Systems and Their Selection in Pharmaceutics and Biopharmaceutics,* Augustijns, P.; Brewster, M. E., Eds. Springer, 2007; pp 151–177. DOI: 10.1007/978-0-387-69154-1_6.
34. Persson, E. M.; Gustafsson, A.-S.; Carlsson, A. S.; Nilsson, R. G.; Knutson, L.; Forsell, P.; Hanisch, G.; Lennernäs, H.; Abrahamsson, B. The effects of food on the dissolution of poorly soluble drugs in human and in model small intestinal fluids. *Pharm. Res*. **2005**, *22* (12), 2141–2151. DOI: 10.1007/s11095-005-8192-x.
35. Persson, E. M.; Nilsson, R. G.; Hansson, G. I.; Löfgren, L. J.; Libäck, F.; Knutson, L.; Abrahamsson, B.; Lennernäs, H. A clinical single-pass perfusion investigation of the dynamic in vivo secretory response to a dietary meal in human proximal small intestine. *Pharm. Res*. **2006**, *23* (4), 742–751. DOI: 10.1007/s11095-006-9607-z.
36. Dressman, J. B.; Amidon, G. L.; Reppas, C.; Shah, V. P. Dissolution testing as a prognostic tool for oral drug absorption: immediate release dosage forms. *Pharm. Res*. **1998**, *15* (1), 11–22. DOI: 10.1023/A:1011984216775.
37. Fotaki, N.; Symillides, M.; Reppas, C. In vitro versus canine data for predicting input profiles of isosorbide-5-mononitrate from oral extended release products on a confidence interval basis. *Eur. J. Pharm. Sci*. **2005**, *24* (1), 115–122. DOI: 10.1016/j.ejps.2004.10.003.
38. Hardy, J. G.; Harvey, W. J.; Sparrow, R. A.; Marshall, G. B.; Steed, K. P.; Macarios, M.; Wilding, I. R. Localization of drug release sites from an oral sustained-release formulation of 5-ASA (Pentasa) in the gastrointestinal tract using gamma scintigraphy. *J. Clin. Pharmacol*. **1993**, *33* (8), 712–718. DOI: 10.1002/j.1552-4604.1993.tb05612.x.
39. Coupe, A. J.; Davis, S. S.; Wilding, I. R. Variation in gastrointestinal transit of pharmaceutical dosage forms in healthy subjects. *Pharm. Res*. **1991**, *8* (3), 360–364. DOI: 10.1023/A:1015849700421.
40. Wen, H.; Park, K. *Oral Controlled Release Formulation Design and Drug Delivery: Theory to Practice*. John Wiley & Sons, 2011.
41. Karuna, D. S.; Rathnam, G.; Ubaidulla, U.; Ganesh, M.; Jang, H. T. Chitosan phthalate: A novel polymer for the multiparticulate drug delivery system for diclofenac sodium. *Adv. Polym. Technol*. **2018**, *37* (6), 2013–2020. DOI: 10.1002/adv.21859.
42. Delrat, P.; Paraire, M.; Jochemsen, R. Complete bioavailability and lack of food-effect on pharmacokinetics of gliclazide 30 mg modified release in healthy volunteers. *Biopharm. Drug Dispos*. **2002**, *23* (4), 151–157. DOI: 10.1002/bdd.303.
43. Batch, J.; Ma, A.; Bird, D.; Noble, R.; Charles, B.; Ravenscroft, P.; Cameron, D. The effects of ingestion time of gliclazide in relationship to meals on plasma glucose, insulin and C-peptide levels. *Eur. J. Clin. Pharmacol*. **1990**, *38* (5), 465–467. DOI: 10.1007/BF02336685.
44. Skripnik, K. K. S.; Riekes, M. K.; Pezzini, B. R.; Cardoso, S. G.; Stulzer, H. K. Investigation of the dissolution profile of gliclazide modified-release tablets using different apparatuses and dissolution conditions. *AAPS PharmSciTech* **2017**, *18* (5), 1785–1794. DOI: 10.1208/s12249-016-0651-7.
45. Patel, S.; Scott, N.; Patel, K.; Mohylyuk, V.; McAuley, W. J.; Liu, F.

Easy to swallow “instant” jelly formulations for sustained release gliclazide delivery. *J. Pharm. Sci*. **2020**, *109* (8), 2474–2484. DOI: 10.1016/j.xphs.2020.04.018.

46. Jantratid, E.; Janssen, N.; Reppas, C.; Dressman, J. B. Dissolution media simulating conditions in the proximal human gastrointestinal tract: an update. *Pharm. Res*. **2008**, *25* (7), 1663–1676. DOI: 10.1007/s11095-008-9569-4.
47. Philip, A. K.; Pathak, K. Osmotic flow through asymmetric membrane: a means for controlled delivery of drugs with varying solubility. *AAPS PharmSciTech* **2006**, *7* (3), 56. DOI: 10.1208/pt070356.